Mar. Res. Indonesia Vol.35, No.1, 2010: 1-7

INVESTIGATION OF THE COASTALLY TRAPPED WAVES IN THE SOUTH OF INDONESIAN ARCHIPELAGO

Asmi Marintan Napitu[1], Kandaga Pujiana[2], and Bayu Priyono[1]
[1]BROK-SEACORM-DKP, Jalan Baru Perancak, Negara, Jembrana, Bali. 82251
[2]Institut Teknologi Bandung, Jalan Ganesha 10 Bandung, 40132
E-mail: asminapitu@gmail.com
Received: 26 January 2010 Accepted: 3 August 2010

ABSTRACT

Analysis of sea level data derived from Jason-1 altimetry satellite reveals the basic characteristics of a coastally trapped wave along the waveguide in the south of Indonesian archipelago. The most robust signatures of the trapped wave are recorded recurrently in the months of May–June. Hovmoller and coherence analysis synonymously agree that the wave propagates at a speed of 2.8–2.9 m/s towards the eastern end of the waveguide. The trapped wave is dependent upon the stratification regime, and a Wentzel–Kramers–Brillouin (WKB) analysis on the stratification profile inferred from several CTD casts indicates that the trapped wave may be classified as a first mode baroclinic wave.

Keywords: Altimetry satellite, Coastally trapped wave, Baroclinic

INTRODUCTION

The use of Sea Level Anomalies (SLA) data, acquired through satellite, to investigate large scale processes such as ocean eddies and equatorial waves, has been made at least since the last two decades. Studies of coastally trapped waves (CTWs) offshore of the Indonesian Archipelago are also not something new. Sprintall *et al.* (2000) suggested that a semiannual coastal Kelvin wave along the south Java coast is from current data, while Syamsudin *et al.* (2005) studied the same subject based on numerical experiments. In this study, the characteristics of a coastally trapped feature are explored at subinertial time scales, using SLA data derived from Jason-1 satellite altimetry. This study is not intended to elucidate in depth of the dynamics of CTWs along the waveguide offshore of the Indonesian Archipelago, but is directed to investigate their basic characteristics such as speeds of propagation and trapping scale.

MATERIALS AND METHODS

The Sea level Anomalies (SLA) data from Jason-1 satellite altimetry are primarily utilized to reveal the footprint of a CTW in our study. The along-track data are then interpolated using an inverse distance weighted (IDW) method to yield the gridded SLA over a region as shown in Figure 1. The principle premise of the IDW method is that the interpolating data are weighted by the inverse of their distance to the interpolated data (Fisher *et al.*, 1987). The SLA data were extended from early January 2004 to late May 2009 with sampling interval of about 10-day. Focus was given to the SLA variability with frequency which was lower than the inertial frequency f, along a transect in offshore west of Sumatra, south of Java, and south of Nusa Tenggara Islands (Figure 1), whereas the f for the study area ranges from 0.6 day–1 to 1.6 day–1 (0.5–1.5 days).

Given the inertial period in the study area is close to tidal periods, we suspected that the tidal signals would be aliased to the SLA data since the 10-day sampling interval of SLA was not high enough to resolve tidal variability. Therefore, we removed the high frequency variance attributed to tidal signatures that might be leaked into the data. Furthermore, examination of the sea level variability along a waveguide from Lombok Strait to internal Indonesian seas (Sprintall *et al.*, 2000; Syamsudin *et al.*, 2005; Pujiana *et al.*, 2009) was not made since the quality of SLA data in the internal of maritime continent is not up to standard

DOI : 10.14203/mri.v35i1.6

(Napitu and Pujiana, 2009). The dominant SLA variability was extracted using a spectral analysis. As for additional data, a stratification profile (Figure 7) off the south Java coast inferred from several Conductivity-Temperature-Depth (CTD) casts is used to estimate the theoretical propagation speed of CTW.

In order to compute the phase speed of CTW, two methods are employed. The first method is the application of the Hovmoller analysis, a time-longitude depiction of SLA variability along a section offshore south of Indonesian Archipelago as given in Figure 1. The second method is the coherence analysis that is simply a cross-power spectrum analysis between two time series (Percival and Walden, 1993). The energy density of the cross-power spectrum is then normalized by a singular power spectrum of each time series to render the amplitude and phase of coherence squared between the two time series in frequency domain as given in the following.

$$coherence^{2} = \frac{\Gamma_{xy}(\omega)^{2}}{\Gamma_{xx}(\omega)\Gamma_{yy}(\omega)} \quad (1)$$

$$phase(\omega) = \tan^{-1}\left(\frac{\mathrm{Im}(\Gamma_{xy}(\omega))}{\mathrm{Re}(\Gamma_{xy}(\omega))}\right) \quad (2)$$

Where Γ is covariance

Given a distance separating locations [L] where the two time series are measured, the speed of a coherent feature [coherence squared > level of significance] oscillating at a certain frequency can be inferred from the phase of coherence analysis as given in eq. 3

$$cp(\omega) = \frac{L}{\frac{\Delta\Phi}{360} X \frac{1}{\omega}} \quad (3)$$

Where $\Delta\Phi$ is the phase difference, is the period of interest, and L denotes the distance separating two locations in calculation.

The phase speed estimates are compared to the theoretical speed of wave propagation factoring in a local stratification profile. Taking fluid at rest and a Boussinesq approximation [vertical velocity varies with depth much more rapidly than density] as the main assumptions, the vertical part of momentum equation can be written:

$$\frac{\partial^{2}}{\partial t^{2}}\nabla^{2}w + N^{2}\nabla_{h}^{2}w = 0 \quad (4)$$

where w and N are vertical velocity [perturbation velocity] and stratification frequency respectively. Subscript h refers to horizontal component of Cartesian coordinate. Assuming the solution of eq. (4) can be decomposed into its vertical and horizontal variability, the perturbation equation and a rigid lid approximation as its boundary condition can be presented as:

$$w = \hat{w}(z)\exp[\,i(kx + ly - \omega t)] \quad (5)$$

$$\frac{\partial^{2}\hat{w}}{\partial z^{2}} + \frac{N^{2}}{c_{n}^{2}}\hat{w} = 0 \quad (6)$$

$$\hat{w}_{z=0=-H} = 0 \quad (7)$$

where c and n are the theoretical phase speed of a baroclinic wave and its corresponding mode number, and H is the water depth. The above set

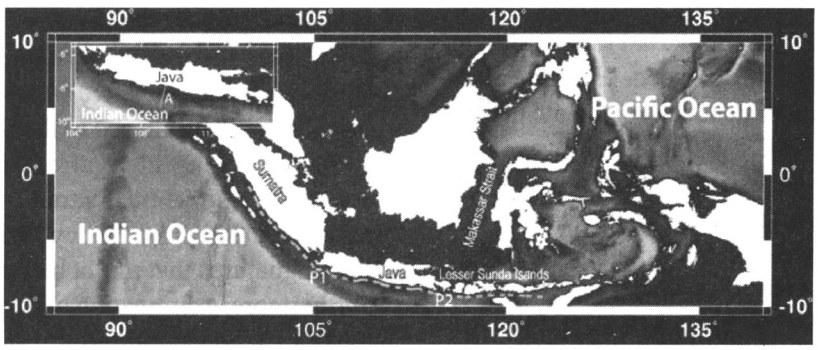

Figure 1. The sea level data along a waveguide in the southern Indonesian archipelago is given as red dashed line, while the offshore section A is given in the inset. P1 and P2 indicate the locations of where the coherence analysis is done.

of equations is an Eigen value problem and can be solved either numerically or analytically. In this study, analytical solution was pursued via the Wentzel–Kramers–Brillouin [WKB] approximation [see Gill (1982) for the derivation], and the analytical solution is given as follows.

$$\hat{w} = N^{-1/2} e^{\pm i\phi} \tag{8}$$

where

$$\phi = \frac{1}{c} \int N dz \tag{9}$$

$$c_n = \int_{-h}^{0} N dz / n\pi \tag{10}$$

To increase the statistical reliability of the spectral and coherence methods, a multitaper analysis is applied. Multitaper analysis multiplies the overlapped and segmented data by several different windows or tapers and subsequently averages the estimates to get an averaged spectrum with a higher degree of freedom or smaller uncertainty (Percival and Walden, 1993). The type of orthogonal window applied in the present study was the discrete prolate spheroidal sequence (Percival and Walden, 1993). The confidence levels specified for the analysis involving spectral and coherence estimates are computed based on the number of degrees of freedom or independent cross-spectral realizations in each frequency band (Thompson, 1979).

RESULTS

Subinertial Variability

Sea level variability along the transect is visually characterized by alternating positive and negative anomalies whose signatures are traceable from offshore west of Sumatra to south of Nusa Tenggara (Figure 2). Figure 2 also shows that there are times when the anomalies are pronounced and periodic along the section such as in the months of December–January, May–June and September–October every year. The strong variance of sea level variability during the monsoon transition period, May–June and September–October, is consistent with the phase of strong semiannual Kelvin waves (Sprintall *et al.*, 2000), while

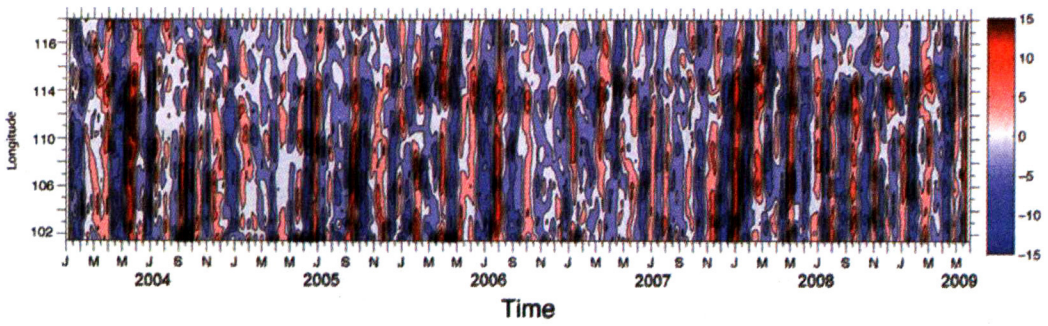

Figure 2. SLA variability at subinertial frequency along a section spanning from offshore West Sumatra to offshore Nusa Tenggara islands and encompassing a period of 5.5 year.

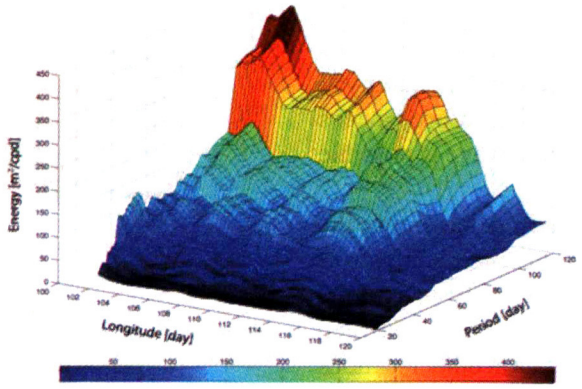

Figure 3. Power spectrum estimate of sea level variability as given in Figure 2.

the significant December–January SLA relates to the oceanic expression of Madden–Julian Oscillations (MJOs) in the form of coastally trapped Kelvin waves (CTWs). In general, the SLA variability along the transect is governed by the intraseasonal oscillations [20–90 days] modulated by the semiannual variability.

Spectrum energy density of the SLA data indeed indicates that the SLA variability is dominated by oscillations within frequency bands of intraseasonal (Figure 3) though the energy resembles a red spectrum shape [energy monotonously increases as period increases] instead of a distinct peak. Figure 3 also shows an interesting aspect: the maximum energy of SLA is offshore West Sumatra, and the energy tends to decay towards offshore Lesser Sunda Islands. This implies that offshore West Sumatra is likely the area where the oscillations originate from, and the oscillating feature dissipates its energy along the waveguide. It is intriguing to figure out whether the dissipation from the SLA spatial variability is indicative of a propagating feature along the waveguide.

Coastally Trapped Waves at Subinertial Frequency

To investigate a propagating feature from the SLA data, to a first approximation, the speeds can be inferred directly from the Time-Longitude plot of sea level variability. For example, focusing on the May–June 2004 of Figure 1 (Figure 4), it can be inferred from the SLA data that there is a trend resembling propagation from the eastern to western end of. A linear approximation of the trend (dashed line in Figure 4), as a rough estimate, signifies that the propagation covers a distance of 2400 km within a period of 10 days implying a phase speed of ~2.9 m/s. Assuming a shallow water wave approximation and the shelf averaged depth of 1000 m, this phase speed is definitely slower than the speeds of barotropic waves such as tides in the region which would transmit their energy at speeds of at least 100 m/s. Therefore, a less speedy wave such as a baroclinic wave is possible to elucidate the variability.

To be more quantitative in determining the speeds of propagation, a coherence analysis is applied to the SLA data. The analysis is done through computation of the coherence between SLA data at a point with SLA data at other locations along the waveguide. As for the initial experiment, two SLA observational points located at P1 and P2 (Figure 1) are chosen as reference points to compute the coherence. The coherence squared between SLA at those to coordinates, as shown in Figure 5, reveals that the variability within a period band of 35–65 is the most coherent. Though other period bands such as 80–90 days and 29–31 days are also slightly above the 95% significance level, it is proposed that they are not convincingly significant and would likely be an expression of 5% statistical error.

The amplitudes of phase differences (Figure 5) between the coherent oscillations observed at two locations indicate two important elements. The first element is that the 36–65 day oscillations have an averaged phase difference of -25° implying that the variability at P1 leads that at P2, i.e. there is a propagation from P1 to P2. Consider the distance between P1 and P2 is 800 km and the period of interest is 45 day, a phase speed computation applying equation would result in a speed of 2.8 m/s which confirms that the speed previously derived from the Hovmoller diagram is acceptable. Another aspect that can be learned from the phase difference is that the shift tends to be smaller as the period increases: the phase difference for oscillation with period of 40 days is bigger than that for oscillation with period of 60 days. If a linear regression method is applied to the phase difference of the most coherent oscillations, the

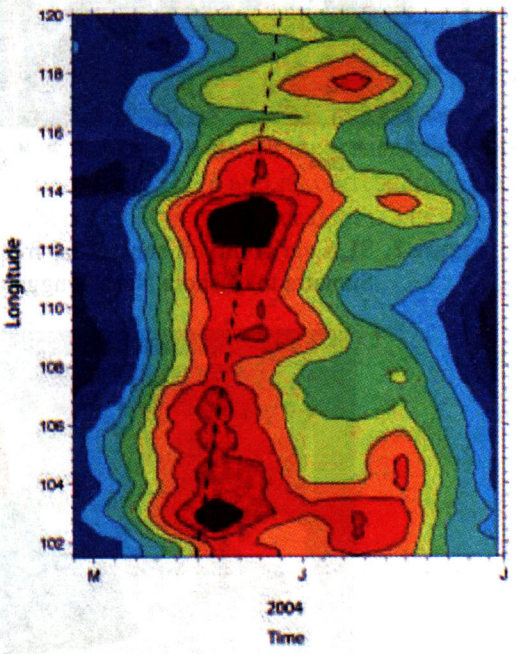

Figure 4. SLA along the transect in Figure 1 for the period of May to June 2004. The dashed line indicates the inclination of SLA signature with respect to longitude.

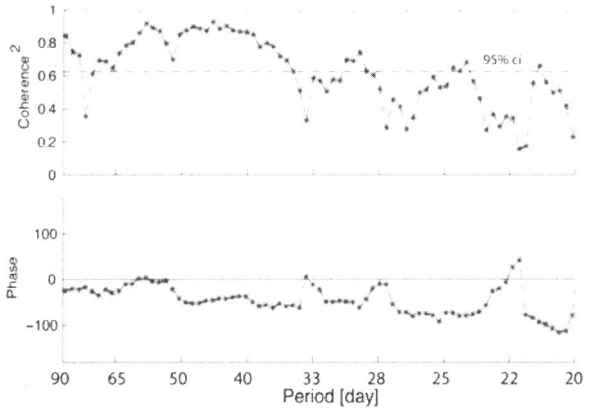

Figure 5. The coherence squared and phase difference between SLA observed at P1 and P2. The dashed line is the 95% significance level.

resulted trend would likely mean that the propagating feature along the wave guide carries its energy with a uniform phase speed irrespective of its period or frequency, i.e. the feature is a non-dispersive wave. Certainly the next question would be more related to what type of baroclinic wave, whether it is a trapped wave with its speed controlled by the stratification regime.

To explore if the propagating feature observed from the SLA data along the waveguide is indeed an expression of a trapped wave, the offshore SLA profile was examined along a transect perpendicular to the coastline located in south of Java (transect A in Figure 1). The discussion is focused on the offshore SLA profile that coincides with the event of robust SLA in May 2004, particularly on May 14th of 2004, and the profile is given in Figure 6.

The offshore SLA profiles (Figure 6) of May 14th indicating that the maximum anomaly is observed near shore and the amplitudes of SLA generally decay away from the shore. The offshore distance of the decaying SLA profile, a distance where the anomaly reaches its zero crossing, is about 160 km. Does the distance exhibit a trapping scale? To examine the trapping scale, the baroclinic Rossby radius of deformation at latitude of -8° was computed, using the following formula (Pedlosky, 2003):

$$R_d = \sqrt{\frac{c}{2\beta}} \qquad (11)$$

Where c is the phase speed we have computed previously, and β is the variation of Coriolis force with latitude. Assigning β=2.7x10-11 and c=2.8 m/s, the theoretical deformation radius is of 227 km which is larger than the observed distance. The inaccuracy in estimate given by the theoretical formula of deformation radius probably indicate that another physical element may play substantial role in defining the trapping scale which is missed from eq. (11), and that factor could be the stratification. The stratification factor can be accommodated into the computation by introducing the Brunt-Väisällä frequency (N2) inferred from several CTD casts obtained along the offshore transect, and its averaged profile within the upper 400 m of water is given in Figure 7.

As it is commonly observed in other open seas region, the maximum N2 is found within thermocline depth where the maximum density variation over depth is located. Nevertheless, for solely computational purpose, the stratification is assumed to be uniform over depth, and its maximum value is chosen as N2=2x10-4 s-2. Given the averaged depth of the bottom is 1000 m, Coriolis force (f), and the meridional distance of the offshore transect from the equator (y), and the assigned N2 as above, the deformation radius can now be calculated using eq. (12), giving the trapping

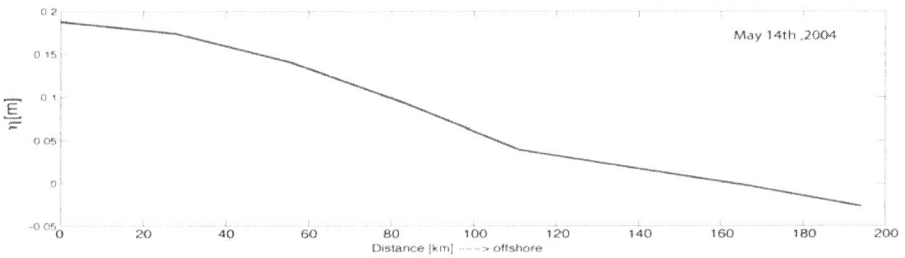

Figure 6. Offshore profile of sea level variability along a transect perpendicular to the South Java coast shown in the Figure 1 inset.

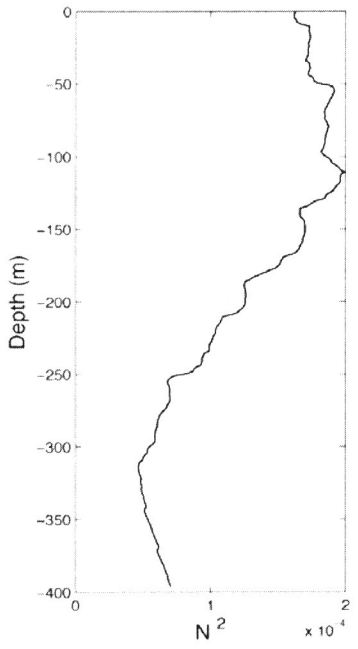

Figure 7. Brunt-Väisällä frequency from CTD casts observed along the offshore transect in the Figure 1 inset.

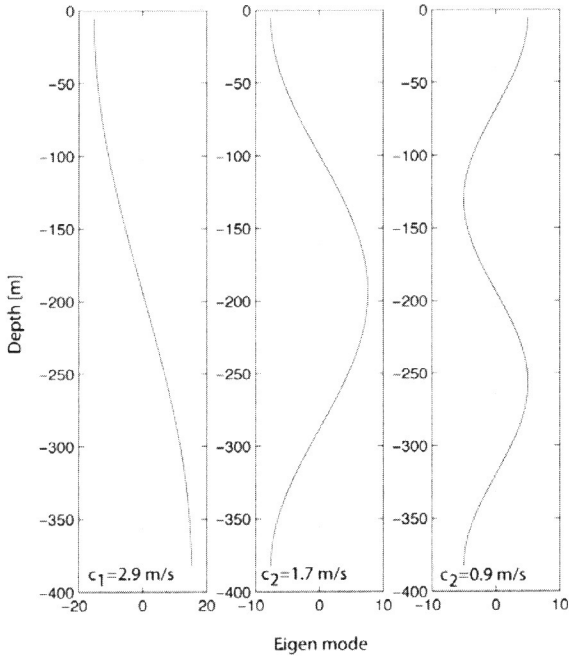

Figure 8. The first three wave modes as for the observed stratification profile as shown in Figure 7.

scale to be of 160 km which is commensurate with the offshore trapping scale observed from the SLA data.

$$R_d = \frac{NH}{f}$$
$$f = \beta y \qquad (12)$$

Therefore, it is argued that the along shelf SLA profile as shown in Figure 6 is the expression of a trapped wave propagating along the waveguide with its offshore distance constrained by the baroclinic Rossby radius of deformation. The stratification could also help gaining insight concerning the theoretical wave phase speed that a water column could possibly sustain. A motion in a water body is considered as a wave motion if its frequency is lower than the strongest stratification value that governs the water body, i.e. a wave frequency should be less than N. In this regard, the speed of wave motion can also be computed, that could theoretically propagate, given certain pattern of stratification. Since the water is stratified or inhomogeneous, a baroclinic wave with its corresponding mode would possibly be excited in the water column. For example, a water column that dynamically can be explained in a two-layer system may have a first mode baroclinic wave as the highest wave mode that possibly propagates over depth. The more layers within the water column, the higher the wave modes that could be ignited in which each wave mode travels case with its corresponding phase speed. By analytically solving eq. (6) with the observed N amplitudes and related boundary conditions, the vertical modes of wave velocity (eigen function) and their corresponding phase speeds (eigen value) can be determined. The first three modes and eigen values are given in Figure 8.

Figure 8 clearly depicts the three most significant vertical wave modes associated with the observed stratification. The first mode has zero crossing at about 200 m depth, while the second and the third modes have multiple zero crossings at other shallower and deeper levels. What counts the most is that the theoretical phase speed of the first baroclinic wave mode is only slightly different from the phase speed inferred from the SLA data: The observed phase speed derived from sea level variability is of 2.8 m/s, while the theoretical phase speed of the first baroclinic wave mode resulted from WKB solution of eq. (6) is 2.9 m/s. Thus, it is physically meaningful and reasonable to conclude that the variability emanating from the western end of the waveguide and propagating eastward is an expression of a first baroclinic wave that is

coastally trapped along the coast of west Sumatra, south Java, and south Nusa Tenggara.

DISCUSSION

Sea level variability observed by Jason-1 altimetry satellite is used to explore the basic characteristics of CTW such as the dominant variability and its phase speed along a waveguide in south of the Indonesian Archipelago. A spectral analysis indicates that the most dominant sea level variability along the waveguide is the intraseasonal variability modulated by the semiannual variations. The robust signatures of sea level variability in the months of May–June are recurrently recorded over the observational period and exhibit a propagating feature with a phase speed of 2.9 m/s from to the western end of the waveguide. A more quantitative coherence method applied to the data observed at two locations offshore of south Java also affirms that there is an energy transfer towards the eastern end of the waveguide with a phase speed of 2.8 m/s. Further analysis to the offshore SLA profile south of Java explains that the propagating feature is a manifestation of a trapped wave whose trapping scale is dependent of stratification. The stratification profile obtained offshore of the south Java also reveals that the propagating feature can be classified as a first mode baroclinic trapped wave.

REFERENCES

Fisher, N.I., T. Lewis and B.J.J. Embleton. 1987. *Statistical Analysis of Spherical Data.* Cambridge University Press, USA 329 pp.

Gill, A.E. 1982. *Atmosphere-Ocean Dynamics.* Academic press, New York, 662 pp.

Napitu, A.M. and K. Pujiana. 2009. Comparison of sea level data derived from tide gauge and altimetry satellite in the Indonesian coastal regions, Journal of Marine Research Indonesia, 4, 47–68.

Pedlosky, J. 2003. *Waves in the Ocean and Atmosphere.* Springer-Verlaag, 276 pp.

Percival, D.B. and A.T. Walden. 1993. *Spectral Analysis for Physical Applications, Multitaper and Conventional Univariate Techniques.* Cambridge University press, USA 583 pp.

Pujiana, K., A.L. Gordon, J. Sprintall, and R.D. Susanto. 2009. Intraseasonal Variability in the Makassar Strait Thermocline. *J. Mar. Res.*, 67(6), 757-777.

Sprintall, J., A.L. Gordon, R. Murtugudde, and R. Dwi Susanto. 2000. *A* Semiannual Indian Ocean forced Kelvin Wave Observed in the Indonesian Seas in May 1997. *J. Geophys.* Res., 105, 17217–17230.

Syamsudin, F., A. Kaneko, and D. B. Haidvogel. 2004. Numerical and Observational Estimates of Indian Ocean Kelvin Wave Intrusion into Lombok Strait. *Geophys.* Res. Lett., *31*, L24307, doi: 10.1029/2004GL021227.

Thompson, R.O.R.Y. 1979. Coherence Significance Levels. *J. Atmos. Sci.*, *36*, 2020–2021.